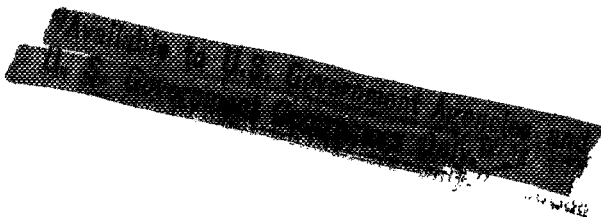


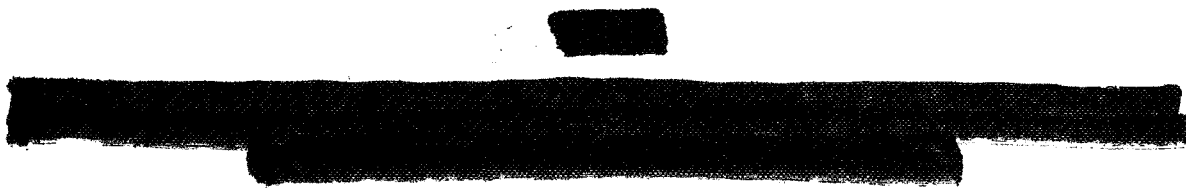
FACILITY FORM 602	N71-71508	78
	(ACCESSION NUMBER)	THRU <i>None</i>
	<i>29</i> (PAGES)	(CODE)
	(NASA CR OR TMX OR AD NUMBER)	(CATEGORY)

RECENT RESEARCH ON THE THEORY OF BONDED JOINTS

Olaf Volkersen



Translation of "Neuere Untersuchungen zur Theorie
der Klebverbindungen."
Wissenschaftliche Gesellschaft für Luft- und
Raumfahrt, Cologne, pp. 1-28, 1963.



Available to U.S. Government Agencies and
U.S. Government Contractors Only

RECENT RESEARCH ON THE THEORY OF BONDED JOINTS

Olaf Volkersen

ABSTRACT

Bonded overlap joints can be used for parts such as torsion tube sheets that are subject to shearing stress, as well as for tension-loaded parts. The stress distribution in the bonding layer depends upon the properties of rigidity of the sheets and of the adhesive. In the first part of these investigations the law of stress distribution for the shear-loaded overlap is developed. In the second part, calculation is made for the tension-loaded double-bonded joint with a formula derived from earlier work in which limiting conditions are better accounted for than formerly.

17021

Author

CONTENTS

1. Introduction
2. Symbols
3. Shearing stress-loaded overlap
4. Tension-loaded double-bonded joint
 - 4.1 Without consideration of peel stresses in the adhesive
 - 4.2 With consideration of the peel stresses in the adhesive
 - 4.3 Variable peel stresses, also in transverse direction
5. Summary
6. References

Section 1. Introduction

Stress distribution in the adhesive layers of bonded overlap joints was first discussed by Arnovljjevic (Ref. 1), 1909, with the assumption of an adhesive elastic only with respect to shear, and later elaborated by von Fillunger (Ref. 2) and by the author (Refs. 3, 4, 5), and applied among other things to rivet joints and plastic deformation. Goland and Reissner (Ref. 6) in simple overlap bonding first considered the bending moment in the bond and calculated the peel stresses in the adhesive.

All works heretofore known present an essential drawback; they neglect limiting conditions on the load-free edges at the joint ends and thereby arrive at a substantially erroneous evaluation of the level of maximum peel stresses. The present work eliminates this defect by assumption of variable normal stress over the thickness of the layer.

In contrast to the heretofore sole known problem of overlap bonding of tension-loaded members, a strong solution is possible by simple means for the distribution of adhesive stresses in shear-loaded members. This solution is discussed in the first part of the present paper. In the second part the calculation of adhesive stresses for the tension-loaded symmetrical double-bonded joint will be presented.

Section 2. Symbols

x, y, z = Coordinates

l = Total length of the overlap

Δ_1, Δ_2 = Sheet thickness

Δ_L = Binder layer thickness

$\bar{x} = \frac{x}{l}$ = Related coordinates

τ_L = Adhesive shearing stress

σ_r = Limit value of the variable supplementary peel stress over $\frac{l}{2}$ the layer thickness

τ_1, τ_2 = Shearing stresses in the sheets outside the overlap

$\sigma_1, \sigma_2, \sigma_0$ = Normal stresses in the sheets outside the overlap

τ_m = Median adhesive shearing stress $\tau_m = \frac{\sigma_1 \cdot \Delta_1}{l}$

$\bar{\tau} = \frac{\tau}{\tau_m}$ = Related stress

$\bar{\sigma} = \frac{\sigma}{\sigma_0}$ = Related stress

$\bar{\sigma}_r = \frac{\sigma_r}{\sigma_0}$ = Related stress

E, G = Modulus of elasticity and modulus of shear of the sheet

E_L, G_L = Modulus of elasticity and modulus of shear of the adhesive

δ = Opposed displacement of the bond

$\bar{\tau}_{max}, \bar{\tau}_0$ = Load increase factor

$\psi = \frac{s_1}{s_2}$ = Sheet thickness ratio

$\psi_L = \frac{s_L}{s}$ = Related layer thickness for symmetrical joint

$\Phi_S = \frac{G_L \cdot \ell^2}{G \cdot s_1 \cdot s_2}$ = Coefficient of rigidity of the joint

$\Phi = \frac{G_L \cdot \ell^2}{E \cdot s_1 \cdot s_2}$ = Coefficient of rigidity of the joint

σ_y = Normal tension in adhesives in the direction of the y-axis and in the middle fiber of the adhesive layer (peel stresses)

$$\omega_S = \sqrt[2]{(1+\psi) \cdot \Phi_S}$$

$$\omega = \sqrt[2]{(1+\psi) \cdot \Phi}$$

$$\lambda_1 = \sqrt[2]{\frac{4+3\psi_L^2}{2} \cdot \frac{G_L \cdot \ell^2}{E \cdot s \cdot s_L}}$$

$$\lambda_2 = \sqrt[2]{8 \cdot \frac{E_L \cdot \ell^2}{G_L \cdot s_L^2}}$$

$$\lambda_3 = \sqrt[4]{3 \cdot \psi_L^2 \cdot \frac{E_L \cdot \ell^4}{E \cdot s \cdot s_L^3}}$$

$$\omega_1 = \lambda_2$$

$$u = \frac{40}{3} \cdot \frac{1+0.6 \cdot \psi_L}{\psi_L^2}$$

$$v = 16 \cdot \frac{\ell^2}{s_L^2}$$

Section 3. Shear-Loaded Overlap

/3

In a shear-loaded joint the bonded parts of the joint exchange shearing stresses. The torsion tubes illustrated in Figure 1 may serve as a model. In the area of the overlap, the angle of slide γ of the joint parts decreases and the opposed displacement δ of the two sheets becomes unequal. If δ_0 indicates the displacement at the left end of

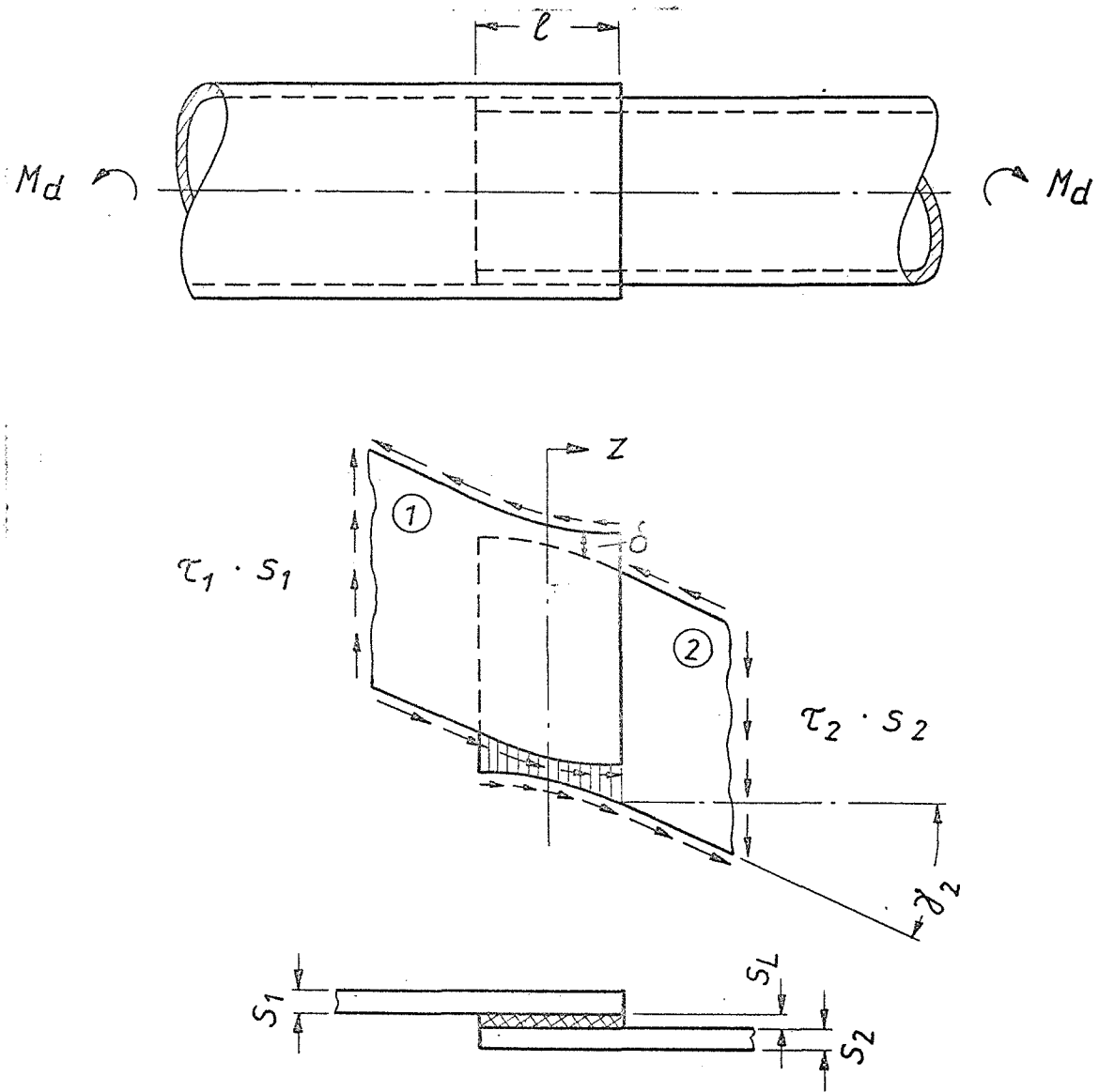


Figure 1. Shear-loaded overlap

the joint and δ_2 the displacement at point z , there then results the general equation of displacement:

$$\delta_z = \delta_0 - \int_{z=-\frac{l}{2}}^z \gamma_1 \cdot dz + \int_{z=-\frac{l}{2}}^z \gamma_2 \cdot dz \quad (1)$$

For the law of elasticity of the adhesive layer of thickness s_L there can then be written:

$$\gamma_L = \frac{\tau_L}{G_L} \quad (2)$$

or

$$\delta_z = \frac{s_L}{G_L} \cdot \tau_{Lz} \quad (3)$$

Furthermore, for the joint parts:

$$\gamma_1 = \frac{\tau_{1z}}{G} = \frac{1}{G} \left[\tau_{10} - \frac{1}{s_1} \int_{z=-\frac{\ell}{2}}^z \tau_{Lz} \cdot dz \right] \quad (4)$$

$$\gamma_2 = \frac{\tau_{2z}}{G} = \frac{1}{G \cdot s_2} \int_{z=-\frac{\ell}{2}}^z \tau_{Lz} \cdot dz \quad (5)$$

By substitution in equation 1 we obtain:

$$\tau_{Lz} = \tau_{L0} + \frac{G_L}{G \cdot s_L} \left[\frac{s_1 + s_2}{s_1 \cdot s_2} \int_{z=-\frac{\ell}{2}}^z \int_{z=-\frac{\ell}{2}}^z \tau_{Lz} \cdot dz \cdot dz - \tau_1 \left(z + \frac{\ell}{2} \right) \right] \quad (6)$$

and after twice repeated differentiation and normalization with:

4

$$\bar{z} = \frac{z}{\ell} \quad \text{and} \quad (7)$$

there results the differential equation:

$$\bar{z}'' = (1 + \psi) \cdot \Phi_s \cdot \bar{z} = \omega_s^2 \cdot \bar{z} \quad (8)$$

Therein

$$\psi = \frac{s_1}{s_2} \quad (9)$$

and

$$\Phi_s = \frac{G_L \cdot l^2}{G \cdot s_1 \cdot s_2} \quad (10)$$

With the general solution of the differential equation:

$$\bar{\tau} = A_1 \cdot \cosh \omega_s \cdot \bar{z} + A_2 \cdot \sinh \omega_s \cdot \bar{z} \quad (11)$$

and with limiting conditions

$$\begin{aligned} 1) & \int_{\bar{z}=-\frac{1}{2}}^{+\frac{1}{2}} \bar{\tau} \cdot d\bar{z} = 1 \\ 2) & \bar{\tau}'_{\bar{z}=-\frac{1}{2}} = -\Phi_s \end{aligned}$$

there is finally obtained:

$$A_1 = \frac{\omega_s}{2} \cdot \frac{1}{\sinh \frac{\omega_s}{2}} \quad (12)$$

and

$$A_2 = \frac{\gamma-1}{\gamma+1} \cdot \frac{\omega_s}{2} \cdot \frac{1}{\cosh \frac{\omega_s}{2}} \quad (13)$$

Thereby the problem is solved. The greatest adhesive shearing stresses appear at the ends of the overlap. They attain a magnitude, especially in symmetrical joints with $s_1 = s_2$, of:

$$\bar{\tau}_0 = \frac{\omega_s}{2} \cdot \coth \frac{\omega_s}{2} = \sqrt{\frac{\Phi_s}{2}} \cdot \coth \sqrt{\frac{\Phi_s}{2}} \quad (14)$$

From equation (14) it is easily recognized that the load increase factor $\bar{\tau}_0$ in long overlaps, approximately at $\Phi_s > 10$, is adequately

15

expressed in the form:

$$\bar{\tau}_0 \approx \sqrt{\frac{\Phi_s}{2}} = \sqrt{\frac{G \cdot l^2}{2 \cdot G \cdot s_1 \cdot s_2}} \quad (15)$$

In long overlaps, therefore, the load increase factor increases in proportion to overlap length, i.e., the absolute value of the adhesive stresses remains independent of it. If the maximum adhesive shearing stress is derived not from the median shear stress, τ_m , but from the shear stress, τ_{Bl} , present in the sheets, for long overlaps it can also be written as:

$$\frac{\tau_o}{\tau_{Bl}} \cong \sqrt{\frac{1}{2} \cdot \frac{G_L}{G} \cdot \frac{s}{s_L}} \quad (16)$$

If this equation is reversed and divided on both sides by the shearing strength of the sheet, the final quality value is:

$$\left(\frac{\tau_{max}}{\tau_B} \right)_{Bl} \cong \frac{\tau_{L8}}{\tau_{B8L}} \cdot \sqrt{2 \cdot \frac{G}{G_L} \cdot \frac{s_L}{s}} \quad (16a)$$

Accordingly, aside from the ratio of strength of the adhesive to sheet material, the final value of the bonded joint, i.e., the maximum shearing stress transferable from one joint part to the other depends upon the ratio of the moduli of slide as well as the ratio of adhesive layer thickness to sheet thickness. The optimal joint, therefore, requires great strength, great layer thickness and slight adhesive rigidity.

Section 4. Tension-Loaded Double-Bonded Joint

/6

4.1 Without consideration of peel stresses in the adhesive

In disregarding the eccentricity of the shearing stresses with respect to the outer sheets, the sliding of the adhesive layer of the joint in Figure 2 at point z can be expressed as follows:

$$\delta_z = \delta_o - \int_{z=-\frac{\ell}{2}}^z \xi_1 \cdot dz + \int_{z=-\frac{\ell}{2}}^z \xi_2 \cdot dz \quad (17)$$

After substitution of the expressions for elongation of the bond as in equation (3) in the preceding section, the following differential equation is obtained:

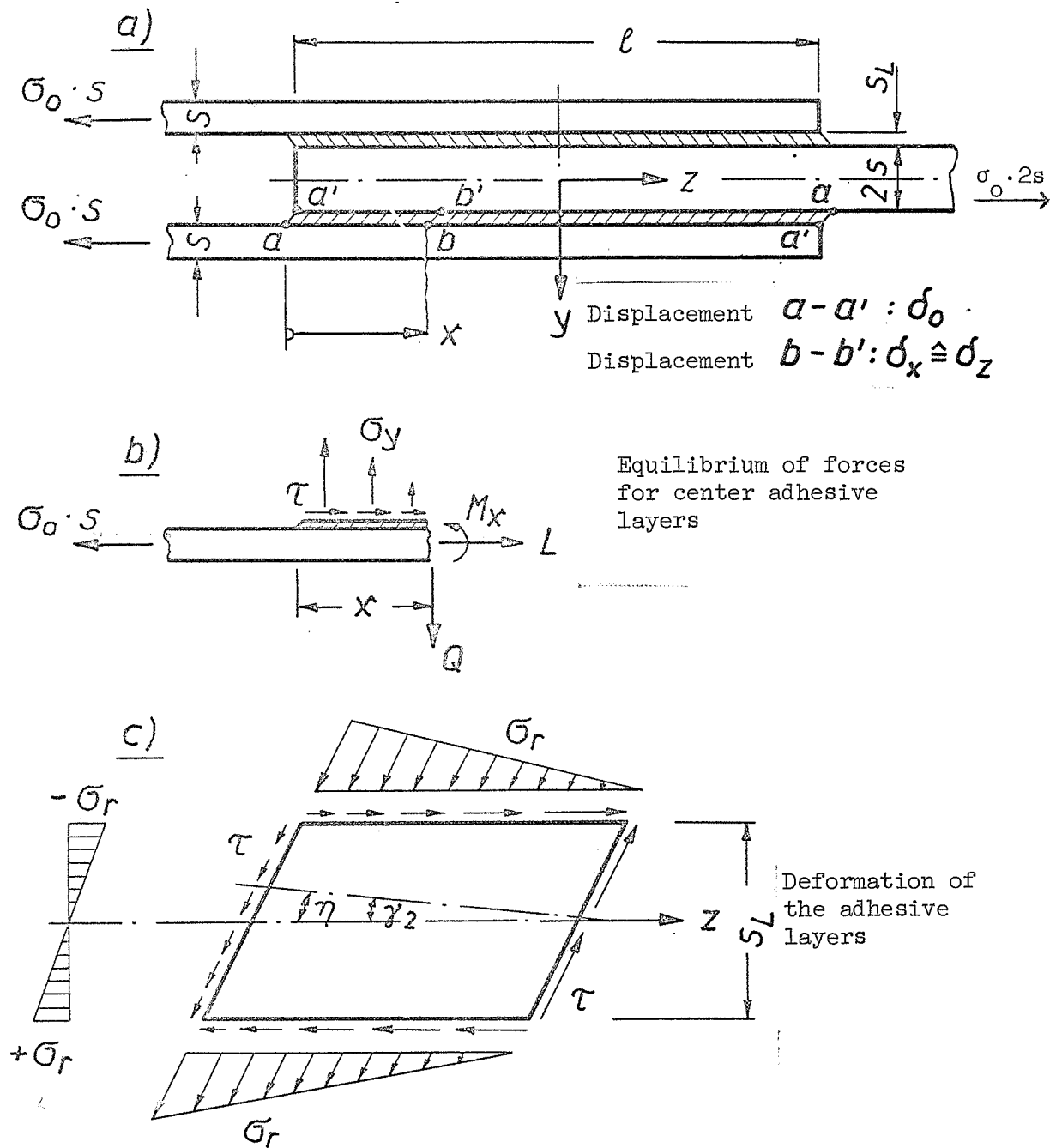


Figure 2. The tension-loaded overlap

$$\bar{\tau}'' = (1 + \psi) \cdot \bar{\Phi} \cdot \bar{\tau} = \omega^2 \cdot \bar{\tau} \quad (18)$$

Therein:

$$\bar{\Phi} = \frac{G \cdot l^2}{E \cdot s \cdot s_L} \quad (19)$$

After introduction of the limiting conditions, for the symmetrical joint with $\psi = \frac{s_1}{s_2} = 1$:

$$\bar{\tau} = \frac{\omega}{2} \cdot \frac{\cosh \omega \bar{z}}{\sinh \frac{\omega}{2}} \quad (20)$$

At the edge, with $\bar{z} = \frac{z}{l} = \pm \frac{1}{2}$, the maximum value of shearing stress, i.e., the load increase coefficient:

$$\bar{\tau}_0 = \frac{\omega}{2} \cdot \coth \frac{\omega}{2} \quad (21)$$

or with sufficiently long overlap:

$$\bar{\tau}_0 \approx \frac{\omega}{2} = \sqrt{\frac{G \cdot l^2}{2 \cdot E \cdot s \cdot s_L}} \quad (22)$$

This value of maximum shear stress at the end of the bond can again be derived from the sheet stress and is then

$$\frac{\tau_0}{\sigma_0} \approx \sqrt{\frac{1}{2} \cdot \frac{G_L \cdot s}{E \cdot s_L}} \quad (23)$$

Finally, the quality factor of the joint will again be:

/7

$$\frac{\sigma_{0 \max}}{\sigma_{B \beta.}} \approx \frac{\tau_{L \beta.}}{\sigma_{B \beta.}} \cdot \sqrt{2 \cdot \frac{E}{G_L} \cdot \frac{s_L}{s}} \quad (23a)$$

4.2 With consideration of the peel stresses in the adhesive

In 4.1, for calculation of the adhesive stresses, only the shear elasticity of the adhesive was taken into consideration. The eccentric attack of the shearing forces on the outer bond was ignored. From the eccentricity of the stress attack, however, as may be seen in Figure 2b, the following equation of moments for a section in the middle adhesive layer is obtained and therewith the equation for the bending line of the outer bond:

$$M_z = \frac{1}{2} (s + s_L) \int_{z=-\frac{\ell}{2}}^z \tau_L \cdot dz + \int_{z=-\frac{\ell}{2}}^z \int_{z=-\frac{\ell}{2}}^z \sigma_y \cdot dz \cdot dz = - \frac{E \cdot s^3}{12} \cdot y'' \quad (24)$$

After introduction of an expression for the elastic deformation y of the adhesive layer in the direction of peel stresses:

$$y = \frac{s_L}{E_L} \cdot \sigma_y \quad (25)$$

and after normalization with

$$\bar{\sigma} = \frac{\sigma_y}{\sigma_0} \quad (26)$$

$$\bar{\tau} = \frac{\tau_L}{\tau_m} \quad (27)$$

as well as introduction of the related variables

$$\bar{z} = \frac{z}{\ell} \quad (28)$$

the differential equation for the peel stresses of the adhesive is obtained:

$$\bar{\sigma}^{IV} + 12 \cdot \frac{E_L \cdot \ell^4}{E \cdot s^3 \cdot s_L} \cdot \bar{\sigma} = -6 (1 + \gamma_L) \cdot \frac{E_L \cdot \ell^2}{E \cdot s \cdot s_L} \cdot \bar{\tau}' \quad (29)$$

A second equation, as in 4.1, is obtained from the shear deformation of the adhesive; after differentiation of equation 17 and with respect to equation 3,

$$\tau_L' = \frac{G_L}{s_L} (\varepsilon_2 - \varepsilon_1) \quad (30)$$

Here, taking into consideration the bending component of the bond elongations, and with $\psi_L = \frac{s_L}{s}$:

$$\varepsilon_1 = \frac{\sigma_0}{E} - \frac{1}{E \cdot s} \int_{-\frac{l}{2}}^z \tau_L \cdot dz - \frac{6}{E \cdot s^2} \left[\frac{s}{2} (1 + \psi_L) \int_{-\frac{l}{2}}^z \tau_L \cdot dz + \int_{-\frac{l}{2}}^z \int_{-\frac{l}{2}}^z \sigma_y \cdot dz \cdot dz \right] \quad (31)$$

$$\varepsilon_2 = \frac{1}{E \cdot s} \int_{-\frac{l}{2}}^z \tau_L \cdot dz \quad (32)$$

After introduction of elongation values in equation 30 and carrying out the required differentiations as well as normalization, the differential equation of shear stresses of the adhesive is:

$$\bar{\tau}''' - (5 + 3 \cdot \psi_L) \cdot \frac{G_L \cdot l^2}{E \cdot s \cdot s_L} \cdot \bar{\tau}' = 6 \cdot \frac{G_L \cdot l^4}{E \cdot s^3 \cdot s_L} \cdot \bar{\sigma} \quad (33)$$

Equations 29 and 33 are coupled. For solution it is advisable to solve equation 29 for $\bar{\tau}'$ and to introduce it into equation 33. There is thus obtained a homogeneous equation 6. Ordering for $\bar{\sigma}$ can be performed without special difficulty. Thereafter, the inhomogeneous equation 33 can be solved for $\bar{\tau}$ also.

The formula corresponds fairly well with that of Goland and Reissner (Ref. 6) for the simple overlap method. The complete calculation is not presented here because the same problem is treated in the following section with an elaborated formula.

4.3 Variable peel stresses, also in transverse direction

/9

With the assumption, as in 4.2, of invariable peel stresses over the thickness of the adhesive layer used also by Goland and Reissner (Ref. 6) in their work on simple overlap bonding, these median values are calculated with fair accuracy, but there is no information concerning the true

maximum value of the peel stresses. Furthermore, the equation does not satisfy the elementary condition of equilibrium:

$$\frac{\partial \tau_z}{\partial z} = \frac{\partial \sigma_y}{\partial y} \quad (34)$$

If, on the contrary, the assumption is made that the peel stresses alter linearly over the layer thickness, then equation 34, as well as the equilibrium of moments in horizontal sections is satisfied, and the shear stresses can disappear at the load-free edges of the bonded layer at the ends of the joint.

The peel stress in the center of the adhesive layer, i.e., in its neutral fibers, is now designated σ_y , while at the upper and lower edge of the adhesive layer, on the contrary, it is designated $\sigma_y \pm \sigma_r$, corresponding to Figure 2b and c. Hence, equation 34 can be written:

$$\sigma_r = \frac{s_L}{2} \cdot \tau_L' \quad (35)$$

Since the shear stresses must disappear at the bond ends, the opposed displacement of the bond here actually reaches its maximum value and the deformation of the adhesive layer from normal stress components σ_r can no longer be ignored. According to Figure 2c, the elongations as a result of σ_r in the lower half of the adhesive layer yield the deformation value:

$$\eta = \int_{y=0}^{y=\frac{s_L}{2}} \varepsilon_y \cdot dy = \frac{\sigma_r}{E_L} \cdot \frac{2}{s_L} \cdot \int_{y=0}^{y=\frac{s_L}{2}} y \cdot dy = \frac{s_L}{4 \cdot E_L} \cdot \sigma_r \quad (36)$$

Deformation value η changes proportionally to the change of σ_r and there is obtained the apparent angle of slide:

$$\beta_z = - \frac{d\eta}{dz} = - \frac{s_L}{4 \cdot E_L} \cdot \frac{d\sigma_r}{dz} = - \frac{s_L}{4 \cdot E_L} \cdot \sigma_r' \quad (37)$$

With equation 35 there will then be

$$\beta_2 = - \frac{s_L^2}{8 \cdot E_L} \cdot \tau_L'' \quad (38)$$

If in addition the angle of slide is calculated from the stress deformation

$$\beta_1 = \frac{\xi_L}{G_L} \quad (39)$$

and thus the opposed displacement of the bond can be expressed as

$$\delta_z = (\beta_1 + \beta_2) \cdot s_L = \frac{s_L}{G_L} \cdot \left[\tau_L - \frac{s_L^2 \cdot G_L}{8 \cdot E_L} \cdot \tau_L'' \right] \quad (40)$$

After differentiation and equalization of equations 17 and 40 there is obtained

$$\tau_L' - \frac{s_L^2 \cdot G_L}{8 \cdot E_L} \cdot \tau_L''' = \frac{G_L}{s_L} \cdot (\xi_2 - \xi_1) \quad (41)$$

Therein ϵ_1 and ϵ_2 are the elongations of the bond at the edge of the

adhesive described in equations 31 and 32. After introduction of these equations and execution of two further differentiations, as well as normalization according to equations 26 to 28, the differential equation for the adhesive shearing stresses is obtained:

$$\bar{\tau}^V - 8 \cdot \frac{E_L \cdot \ell^2}{G_L \cdot s_L^2} \cdot \bar{\tau}''' + 40(1 + 0,6 \psi_L) \frac{E_L \cdot \ell^4}{E \cdot s \cdot s_L^3} \cdot \bar{\tau}' = - 48 \cdot \frac{E_L \cdot \ell^6}{E \cdot s^3 \cdot s_L^3} \cdot \bar{\sigma} \quad (42)$$

In addition, the differential equation 29 derived in section 4.2 again appears for the peel stresses.

Now equation 29 is solved for $\bar{\tau}'$, further differentiated and introduced into equation 42. Thereby, finally, the following homogeneous equation for $\bar{\sigma}$ is developed:

$$\begin{aligned} \bar{\sigma}^{VIII} - 8 \cdot \frac{E_L \cdot \ell^2}{G_L \cdot s_L^2} \cdot \bar{\sigma}^{VI} + 40(1 + 0,6 \psi_L + 0,3 \psi_L^2) \cdot \frac{E_L \cdot \ell^4}{E \cdot s \cdot s_L^3} \cdot \bar{\sigma}^{IV} \\ - 96 \cdot \frac{E_L \cdot \ell^6}{E \cdot G_L \cdot s^3 \cdot s_L^3} \cdot \bar{\sigma}^{II} + 192 \cdot \left(\frac{E_L \cdot \ell^4}{E \cdot s^2 \cdot s_L^2} \right)^2 \cdot \bar{\sigma} = 0 \end{aligned} \quad (43)$$

The solution of this differential equation, with consideration of only the antisymmetrical members, is

/11

$$\bar{\sigma} = C_1 \sinh \lambda_1 \bar{z} + C_2 \sinh \lambda_2 \bar{z} + C_3 \sinh \lambda_3 \bar{z} \cdot \cos \lambda_3 \bar{z} + C_4 \cosh \lambda_3 \bar{z} \cdot \sinh \lambda_3 \bar{z} \quad (44)$$

with

$$\lambda_1 = \sqrt[2]{\frac{4+3\psi_L^2}{2} \cdot \frac{G_L \cdot \ell^2}{E \cdot s \cdot s_L}} \quad (45)$$

$$\lambda_2 = \sqrt[2]{8 \cdot \frac{E_L \cdot \ell^2}{G_L \cdot s_L^2}} \quad (46)$$

$$\lambda_3 = \sqrt[4]{3\psi_L^2 \cdot \frac{E_L \cdot \ell^4}{E \cdot s \cdot s_L^3}} \quad (47)$$

In the solution of the characteristic equations related to equation 43 only the members most important for the result were used. The minor expressions relating to the temporary principal member were disregarded.

For determination of the integration constants of equation 44 the following limiting conditions are obtained:

1) With the assumption that the bonds outside the joint are free of bending moments, from equation 24:

$$\frac{1}{2}(s + s_L) \cdot \tau_m \cdot \ell + \int_{-\frac{\ell}{2}}^{+\frac{\ell}{2}} \int_{-\frac{\ell}{2}}^{+\frac{\ell}{2}} \bar{\sigma}_y \cdot d\bar{z} \cdot d\bar{z} = 0$$

or after normalization

$$\int_{-\frac{1}{2}}^{+\frac{1}{2}} \int_{-\frac{1}{2}}^{+\frac{1}{2}} \bar{\sigma} \cdot d\bar{z} \cdot d\bar{z} = - \frac{1}{2} (1 + \psi_L) \left(\frac{s}{\ell} \right)^2 \quad (48)$$

2) For $\bar{z} = \frac{1}{2}$, the bending moment in the outer bond equals zero and thereby $y'' = 0$, and because of equation 25 also

$$\bar{\sigma}''''_{\bar{z}=\frac{1}{2}} = 0 \quad (49)$$

3) By differentiation of equation 24 there is obtained

$$\frac{\lambda}{2} (1 + \gamma_L) \cdot \tau_L + \int_{-1}^{\bar{z}} \bar{\sigma}_y \cdot dz = - \frac{E \cdot \lambda^3}{12} \cdot y'''$$

However, since in place of $\bar{z} = -\frac{1}{2}$, the shear stress $\tau_{L0} = 0$ and the integral of the left side disappears, $y''' = 0$ must also be obtained, and thereby $\bar{\sigma}'''' = 0$. Also at $\bar{z} = +\frac{1}{2}$:

$$\bar{\sigma}''''_{\bar{z}=\frac{1}{2}} = 0 \quad (50)$$

4) From equation 41 after introduction of equations 31 and 32 at $\bar{z} = -\frac{1}{2}$:

$$\tau_L' - \frac{\lambda_L^2 \cdot G_L}{8 \cdot E_L} \cdot \tau_L''' = - \frac{G_L}{\lambda_L} \cdot \bar{\sigma}_0$$

Because of the antisymmetrical structure of the solution for $\bar{\sigma}$ the sign of the right side must be reversed at $\bar{z} = +\frac{1}{2}$. Then, at this point after introduction of equation 29 and after normalization

$$\bar{\sigma}^{VI} - \lambda_2^2 \cdot \bar{\sigma}^{IV} - 4 \cdot \lambda_2^2 \cdot \lambda_3^4 \cdot \bar{\sigma} = \frac{16}{3} \cdot \frac{1 + \gamma_L}{\gamma_L^2} \cdot \left(\frac{\lambda}{l}\right)^2 \cdot \lambda_2^8 \quad (51)$$

After introduction of the limiting conditions the following schema of equations for determination of the four integration constants C_i of equation 44 are obtained

$$\begin{pmatrix} a_{11} & a_{12} & a_{13} & a_{14} \\ a_{21} & a_{22} & a_{23} & a_{24} \\ a_{31} & a_{32} & a_{33} & a_{34} \\ a_{41} & a_{42} & a_{43} & a_{44} \end{pmatrix} \cdot \begin{pmatrix} c_1 \\ c_2 \\ c_3 \\ c_4 \end{pmatrix} = \begin{pmatrix} a_{15} \\ 0 \\ 0 \\ a_{45} \end{pmatrix} \quad (52)$$

Therein for coefficients a_{ik} the following equations are valid:

$$\left\{ \begin{aligned} a_{11} &= \frac{1}{\lambda_1^2} \cdot \left(\lambda_1 \cdot \cosh \frac{\lambda_1}{2} - 2 \cdot \sinh \frac{\lambda_1}{2} \right) \\ a_{12} &= \frac{1}{\lambda_2^2} \cdot \left(\lambda_2 \cdot \cosh \frac{\lambda_2}{2} - 2 \cdot \sinh \frac{\lambda_2}{2} \right) \\ a_{13} &= \frac{1}{2 \cdot \lambda_3^2} \left[\lambda_3 \left(\cosh \frac{\lambda_3}{2} \cdot \cos \frac{\lambda_3}{2} + \sinh \frac{\lambda_3}{2} \cdot \sin \frac{\lambda_3}{2} \right) - 2 \cdot \cosh \frac{\lambda_3}{2} \cdot \sin \frac{\lambda_3}{2} \right] \\ a_{14} &= \frac{1}{2 \cdot \lambda_3^2} \left[\lambda_3 \left(\sinh \frac{\lambda_3}{2} \cdot \sin \frac{\lambda_3}{2} - \cosh \frac{\lambda_3}{2} \cdot \cos \frac{\lambda_3}{2} \right) + 2 \cdot \sinh \frac{\lambda_3}{2} \cdot \cos \frac{\lambda_3}{2} \right] \\ a_{15} &= \frac{1 + \gamma_L}{2} \cdot \left(\frac{s}{l} \right)^2 \end{aligned} \right. \quad (53.1)$$

/13

$$\left\{ \begin{aligned} a_{21} &= \frac{1}{2} \cdot \left(\frac{\lambda_1}{\lambda_3} \right)^2 \cdot \sinh \frac{\lambda_1}{2} \\ a_{22} &= \frac{1}{2} \cdot \left(\frac{\lambda_2}{\lambda_3} \right)^2 \cdot \sinh \frac{\lambda_2}{2} \\ a_{23} &= - \cosh \frac{\lambda_3}{2} \cdot \sin \frac{\lambda_3}{2} \\ a_{24} &= \sinh \frac{\lambda_3}{2} \cdot \cos \frac{\lambda_3}{2} \end{aligned} \right. \quad (53.2)$$

$$\left\{ \begin{array}{l} a_{31} = \frac{1}{2} \cdot \left(\frac{\lambda_1}{\lambda_3} \right)^3 \cdot \cosh \frac{\lambda_1}{2} \\ a_{32} = \frac{1}{2} \cdot \left(\frac{\lambda_2}{\lambda_3} \right)^3 \cdot \cosh \frac{\lambda_2}{2} \\ a_{33} = -\cosh \frac{\lambda_3}{2} \cdot \cos \frac{\lambda_3}{2} - \sinh \frac{\lambda_3}{2} \cdot \sin \frac{\lambda_3}{2} \\ a_{34} = \cosh \frac{\lambda_3}{2} \cdot \cos \frac{\lambda_3}{2} - \sinh \frac{\lambda_3}{2} \cdot \sin \frac{\lambda_3}{2} \end{array} \right. \quad (53.3)$$

$$\left\{ \begin{array}{l} a_{41} = 4 \cdot \sinh \frac{\lambda_1}{2} \\ a_{42} = 4 \cdot \sinh \frac{\lambda_2}{2} \\ a_{43} = -8 \cdot \left(\frac{\lambda_3}{\lambda_2} \right)^2 \cdot \cosh \frac{\lambda_3}{2} \cdot \sin \frac{\lambda_3}{2} \\ a_{44} = 8 \cdot \left(\frac{\lambda_3}{\lambda_2} \right)^2 \cdot \sinh \frac{\lambda_3}{2} \cdot \cos \frac{\lambda_3}{2} \\ a_{45} = -\frac{16}{3} \cdot \frac{1+\psi_L}{\psi_L^2} \cdot \left(\frac{\lambda}{\ell} \right)^2 \cdot \frac{\lambda_3^4}{\lambda_2^2} \end{array} \right. \quad (53.4)$$

With solution of the matrix of equation 52, the peel stresses $\bar{\sigma}$ in the midplane of the adhesive layer are known. Now the shearing stresses can also be calculated from equation 42. This equation is first written with equations 45 to 47 and with abbreviations

$$\mu = \frac{40}{3} \cdot \frac{1+0.6\psi_L}{\psi_L^2} \quad (54)$$

$$\nu = 16 \cdot \left(\frac{\ell}{\lambda_2} \right)^2 \quad (55)$$

in the described form

$$\bar{c}^V - \lambda_2^2 \cdot \bar{c}''' + \mu \cdot \lambda_3^4 \cdot \bar{c}' = -\nu \cdot \lambda_3^4 \cdot \bar{\sigma} \quad (56)$$

The complete solution of this equation is composed of both a special solution \bar{c}_i of the inhomogeneous equation and of the general

solution \bar{c}_h of the homogeneous remainder of the equation. It is:

$$\bar{\epsilon} = \bar{\epsilon}_i + \bar{\epsilon}_h \quad (57)$$

A solution of the inhomogeneous equation is easily recognized in the form:

$$\begin{aligned} \bar{\epsilon}_i = & K_1 \cdot \frac{1}{\lambda_1} \cdot \cosh \lambda_1 \bar{z} + K_2 \cdot \frac{1}{\lambda_2} \cdot \cosh \lambda_2 \bar{z} \\ & + \frac{1}{2\lambda_3} \left[K_3 \left(\cosh \lambda_3 \bar{z} \cdot \cos \lambda_3 \bar{z} + \sinh \lambda_3 \bar{z} \cdot \sin \lambda_3 \bar{z} \right) + K_4 \left(\sinh \lambda_3 \bar{z} \cdot \sin \lambda_3 \bar{z} - \cosh \lambda_3 \bar{z} \cdot \cos \lambda_3 \bar{z} \right) \right] \end{aligned} \quad (58)$$

Coefficients K_i are determined by introduction of the differential quotients of equation 58 into equation 56 by comparison of coefficients:

$$\left\{ \begin{aligned} K_1 &= - \frac{v \cdot \lambda_3^4}{u \cdot \lambda_3^4 - \lambda_1^2 \lambda_2^2 + \lambda_1^4} \cdot c_1 \\ K_2 &= - \frac{v}{u} \cdot c_2 \\ K_3 &= - v \cdot \frac{2 \left(\frac{\lambda_2}{\lambda_3} \right)^2 \cdot c_4 + (u-4) \cdot c_3}{4 \cdot \left(\frac{\lambda_2}{\lambda_3} \right)^4 + (u-4)^2} \\ K_4 &= v \cdot \frac{2 \left(\frac{\lambda_2}{\lambda_3} \right)^2 \cdot c_3 - (u-4) \cdot c_4}{4 \cdot \left(\frac{\lambda_2}{\lambda_3} \right)^4 + (u-4)^2} \end{aligned} \right. \quad (59)$$

The solution of the homogeneous equation remainder in equation 56 must also be symmetrical in \bar{z} and is thereby:

$$\bar{\epsilon}_h = D_1 + D_2 \cdot \cosh \omega_1 \bar{z} + D_3 \cdot \cosh \omega_2 \bar{z} \quad (60)$$

From the characteristic equation it is calculated that

$$\omega_1 = \sqrt[2]{8 \cdot \frac{E_L \cdot l^2}{G_L \cdot s_L^2}} = \lambda_2 \quad (61)$$

$$\omega_2 = \sqrt[2]{(5+3\gamma_2) \cdot \frac{G_L \cdot l^2}{E_L \cdot s_L}} \quad (62)$$

For determination of coefficients D_i in equation 60 the following limiting conditions are obtained:

/15

- 1) The shearing stress transfers the outer load, therefore:

$$\int_{z=-\ell/2}^{z=+\ell/2} \tau_L \cdot dz = G_0 \cdot \Delta$$

or normalized

$$\int_{-1/2}^{+1/2} \bar{\tau} \cdot d\bar{z} = 1 \quad (63)$$

- 2) For $\bar{z} = \frac{1}{2}$:

(64)

3) From equation 41 at $\bar{z} = \frac{1}{2}$ (see also fourth limiting condition for $\bar{\sigma}$)

$$\tau_L' - \frac{\Delta^2 \cdot G_L}{8 \cdot E_L} \cdot \tau_L''' = \frac{G_L}{\Delta} \cdot \frac{G_0}{E}$$

or after normalization

$$\bar{\tau}' - \frac{1}{\omega_1^2} \cdot \bar{\tau}''' = \frac{\omega_2^2}{5+3\psi_L} \quad (65)$$

After satisfying these limiting conditions by the complete solution of equation 57 the following system of equations for D_i is obtained:

$$\begin{pmatrix} a_{11} & a_{12} & a_{13} \\ a_{21} & a_{22} & a_{23} \\ 0 & 0 & a_{33} \end{pmatrix} \cdot \begin{pmatrix} D_1 \\ D_2 \\ D_3 \end{pmatrix} = \begin{pmatrix} a_{14} \\ a_{24} \\ a_{34} \end{pmatrix} \quad (66)$$

with the coefficients:

$$\begin{cases} a_{11} = 1 \\ a_{12} = \frac{2}{\omega_1} \cdot \sinh \frac{\omega_1}{2} \\ a_{13} = \frac{2}{\omega_2} \cdot \sinh \frac{\omega_2}{2} \\ a_{14} = 1 - \left[\frac{2}{\lambda_1^2} \cdot \sinh \frac{\lambda_1}{2} \cdot K_1 + \frac{2}{\lambda_2^2} \cdot \sinh \frac{\lambda_2}{2} \cdot K_2 + \frac{1}{\lambda_3^2} \cdot \cosh \frac{\lambda_3}{2} \cdot \sinh \frac{\lambda_3}{2} \cdot K_3 \right] \end{cases} \quad (67.1)$$

/16

$$\begin{cases} a_{21} = 1 \\ a_{22} = \cosh \frac{\omega_1}{2} \\ a_{23} = \cosh \frac{\omega_2}{2} \\ a_{24} = - \left[\frac{1}{\lambda_1} \cdot \cosh \frac{\lambda_1}{2} \cdot K_1 + \frac{1}{\lambda_2} \cdot \cosh \frac{\lambda_2}{2} \cdot K_2 + \frac{1}{2\lambda_3} \cdot \left(\cosh \frac{\lambda_3}{2} \cdot \cosh \frac{\lambda_3}{2} + \sinh \frac{\lambda_3}{2} \cdot \sinh \frac{\lambda_3}{2} \right) \cdot K_3 - \frac{1}{2\lambda_3} \cdot \left(\cosh \frac{\lambda_3}{2} \cdot \cosh \frac{\lambda_3}{2} - \sinh \frac{\lambda_3}{2} \cdot \sinh \frac{\lambda_3}{2} \right) \cdot K_4 \right] \end{cases} \quad (67.2)$$

$$\begin{cases} a_{31} = 0 \\ a_{32} = 0 \\ a_{33} = \omega_2 \cdot \left(1 - \frac{\omega_2^2}{\omega_1^2} \right) \cdot \sinh \frac{\omega_2}{2} \\ a_{34} = \frac{\omega_2^2}{5 + 3 \cdot \psi_L} - \left[\left(1 - \frac{\lambda_1^2}{\lambda_2^2} \right) \cdot \sinh \frac{\lambda_1}{2} \cdot K_1 + \left(\sinh \frac{\lambda_3}{2} \cdot \cosh \frac{\lambda_3}{2} + 2 \cdot \frac{\lambda_3^2}{\lambda_2^2} \cdot \cosh \frac{\lambda_3}{2} \cdot \sinh \frac{\lambda_3}{2} \right) \cdot K_3 + \left(\cosh \frac{\lambda_3}{2} \cdot \sinh \frac{\lambda_3}{2} - 2 \cdot \frac{\lambda_3^2}{\lambda_2^2} \cdot \sinh \frac{\lambda_3}{2} \cdot \cosh \frac{\lambda_3}{2} \right) \cdot K_4 \right] \end{cases} \quad (67.3)$$

After solution of this system of equations the shearing stresses are also known and there is still only the unequal factor $\bar{\sigma}_r$ of the peel

stress to be calculated from equation 35. After normalization and introduction of equation 57 there is, finally:

$$\bar{\sigma}_r = \pm \frac{1}{2} \cdot \frac{s \cdot s_L}{l^2} \left(D_2 \cdot \omega_1 \cdot \sinh \omega_1 \bar{z} + D_3 \cdot \omega_2 \cdot \sinh \omega_2 \bar{z} + K_1 \cdot \sinh \lambda_1 \bar{z} + K_2 \cdot \sinh \lambda_2 \bar{z} + K_3 \cdot \sinh \lambda_3 \bar{z} \cdot \cosh \lambda_3 \bar{z} + K_4 \cdot \cosh \lambda_3 \bar{z} \cdot \sinh \lambda_3 \bar{z} \right) \quad (68)$$

The results of a first series of numerical calculation are shown in Figures 3 to 7¹.

These calculations with respect to distribution of shearing stress over the length of the seam yield only slight deviations from the approximation repeated in Section 4.1 (Refs. 3, 4, 5). The stress increase factor, especially in long joints, remains somewhat below the theoretical value because the shearing stress maximum is set back slightly from the end of the bond. At the bond end the shearing stress in the adhesive zone is zero.

In addition to shearing stresses, there are also, however, peel stresses of such notable magnitude that dimensioning of bonds to shear is of less importance than dimensioning with respect to peel. The greatest peel stresses occur in a quite narrow, almost punctiform region, at the ends of the bond (Point a in Figure 2a). /17

A comparison of calculated results in Figure 8 with photostress investigations of Stier (Ref. 7) supports the calculation of a double-bonded joint very well.

Section 5. Summary

An investigation of stress distribution in an adhesive layer of overlap joints of shear-loaded joint parts for sheet connections to spar webs or torsion pipes leads to similar relationships, as they have long been recognized as approximations for tension-loaded overlap joints. The quality grade of these joints increases with adhesive strength and with layer thickness and decreases with respect to the modulus of elasticity or modulus of slide of the adhesive.

For symmetrical tension-loaded double-bonded joints calculations are made with an expanded formula that fulfills the limiting conditions

¹For the numerical working out of the calculations the Fa. Zuse KG kindly placed at our disposal in its Hamburg computer center a type Z23 computer. For his collaboration in the programming in Alcorette code, I am grateful to Dr. Kunsemüller.

a Kunsemüller.

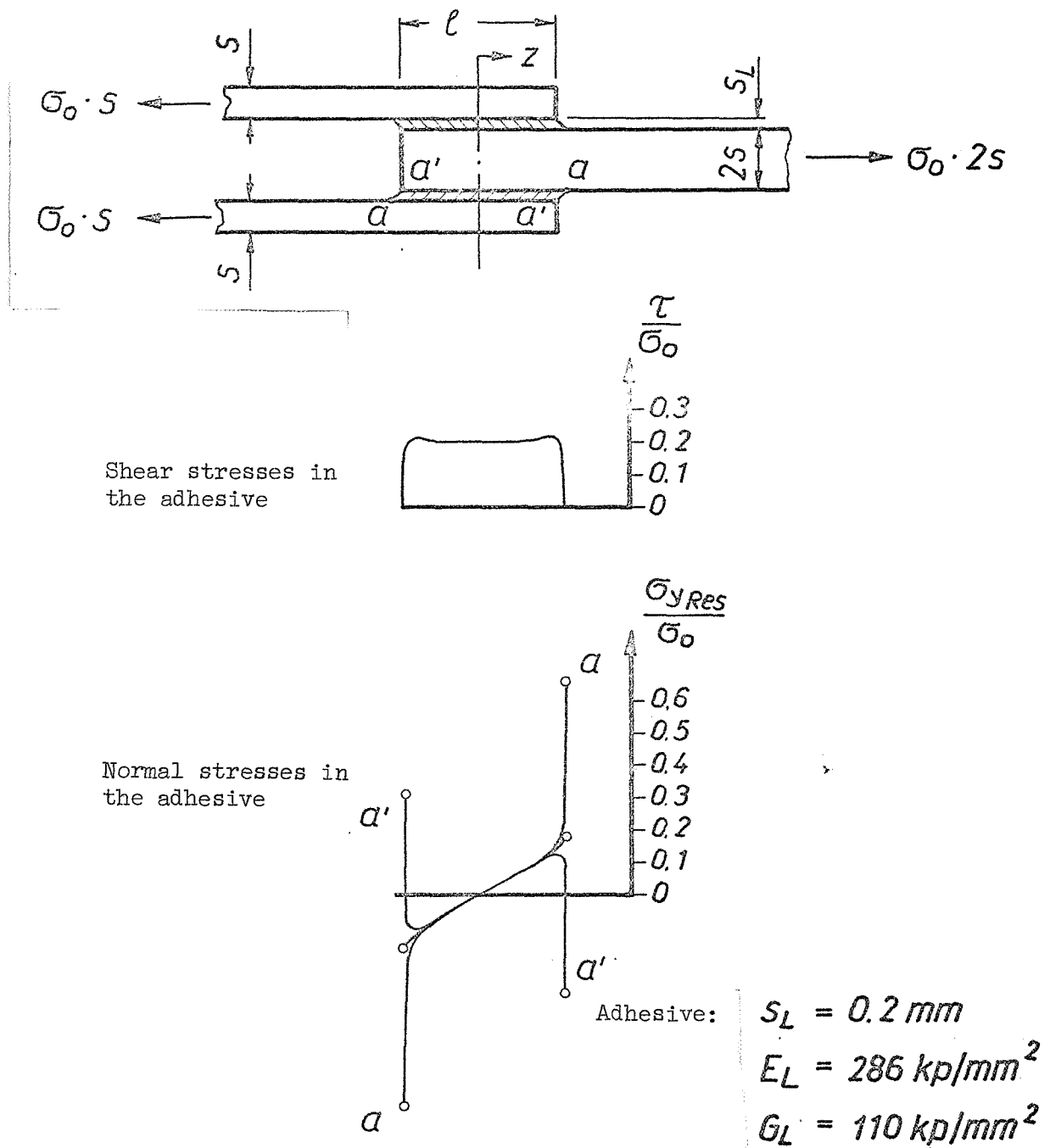


Figure 3

Double-bonded joint: $l/s = 5$
 Steel sheet, synthetic resin adhesive: $s/s_L = 4$

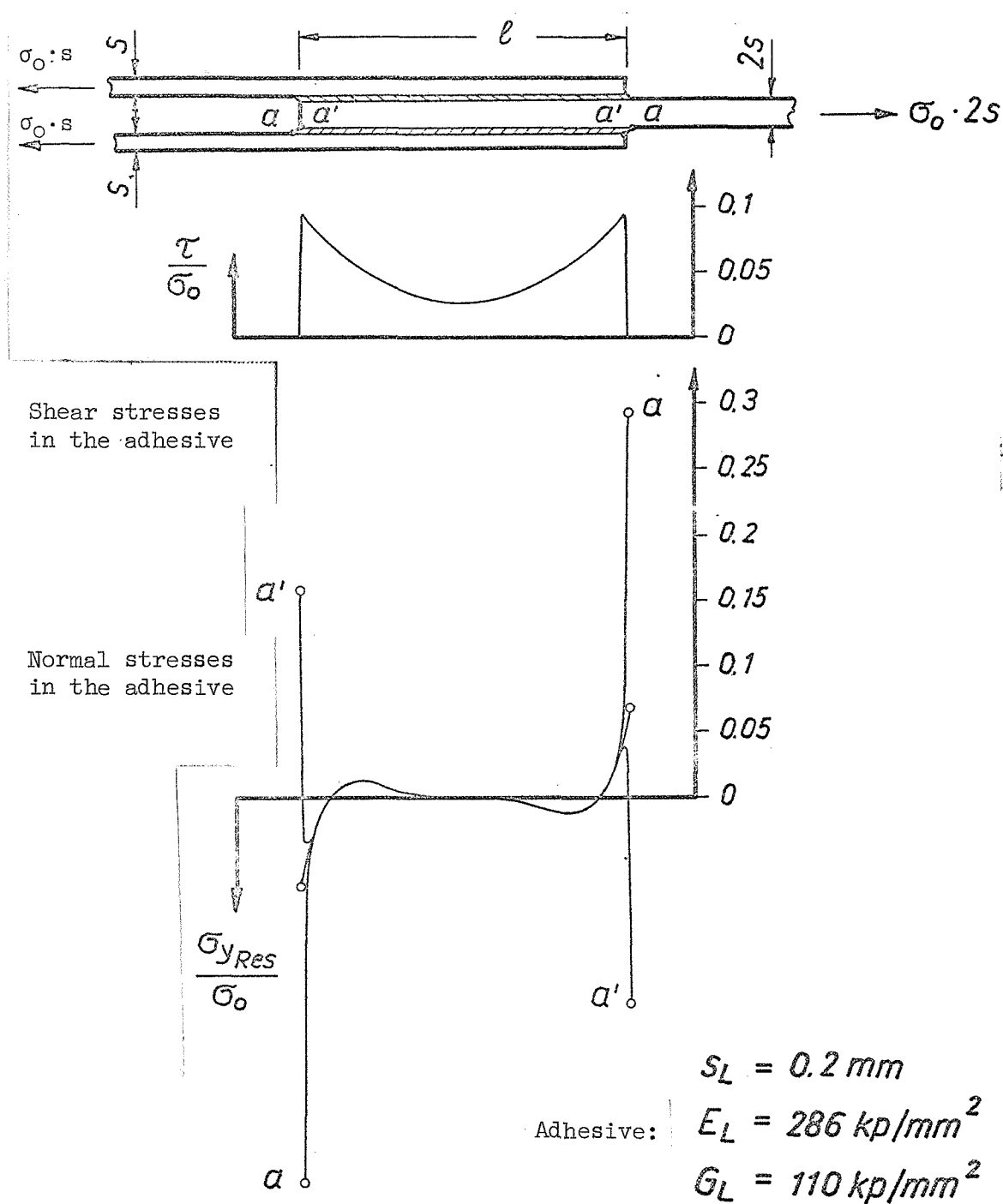


Figure 4

Double-bonded joint: $1/s = 20$

Steel sheet, synthetic resin adhesive: $s/s_L = 4$

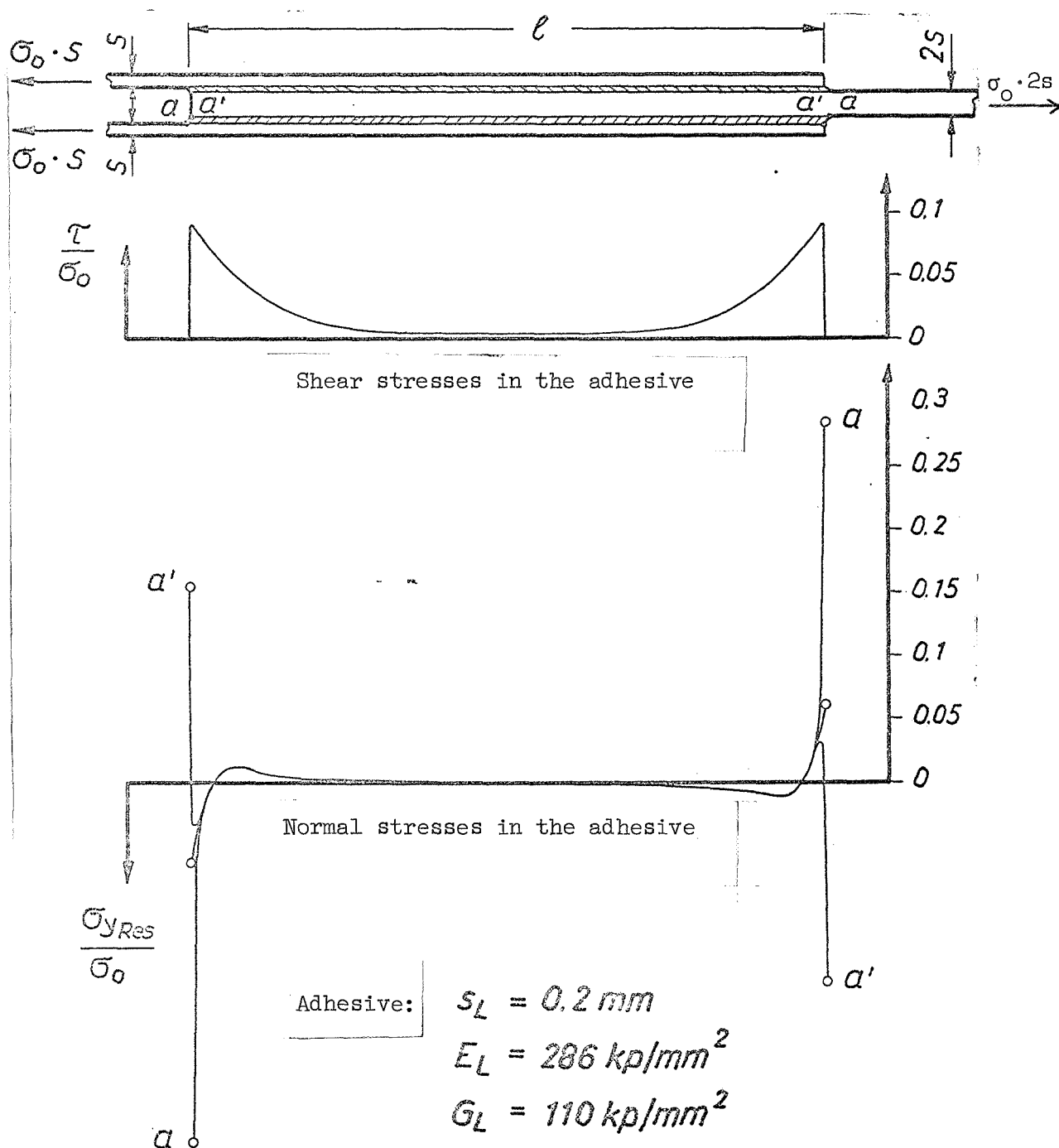


Figure 5

Double-bonded joint: $1/s = 50$
 Steel sheet, synthetic resin adhesive: $s/s_L = 4$

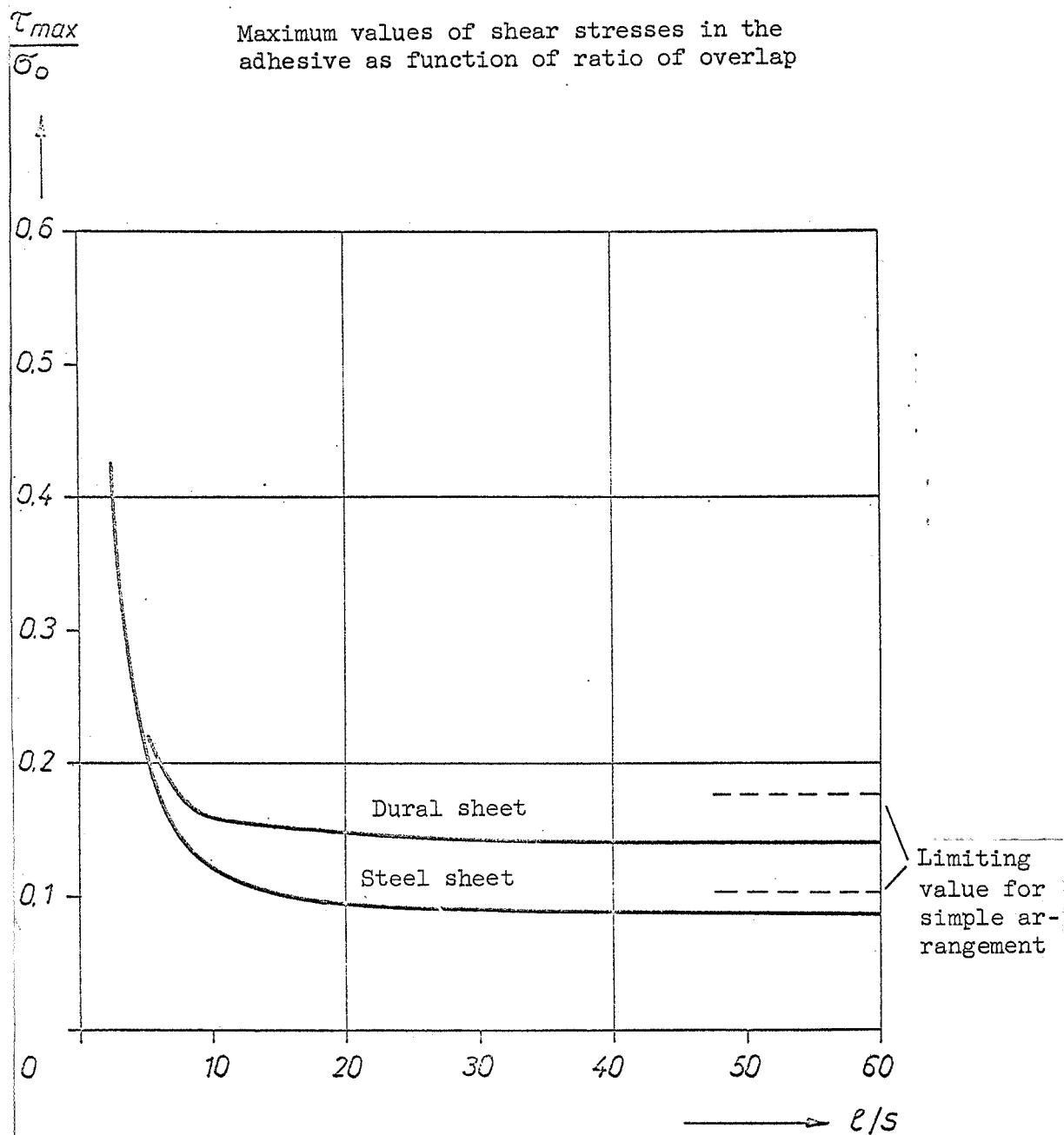


Figure 6

Double-bonded joint: $s = 0.8$ mm
 Synthetic resin adhesive: $s_L = 0.2$ mm

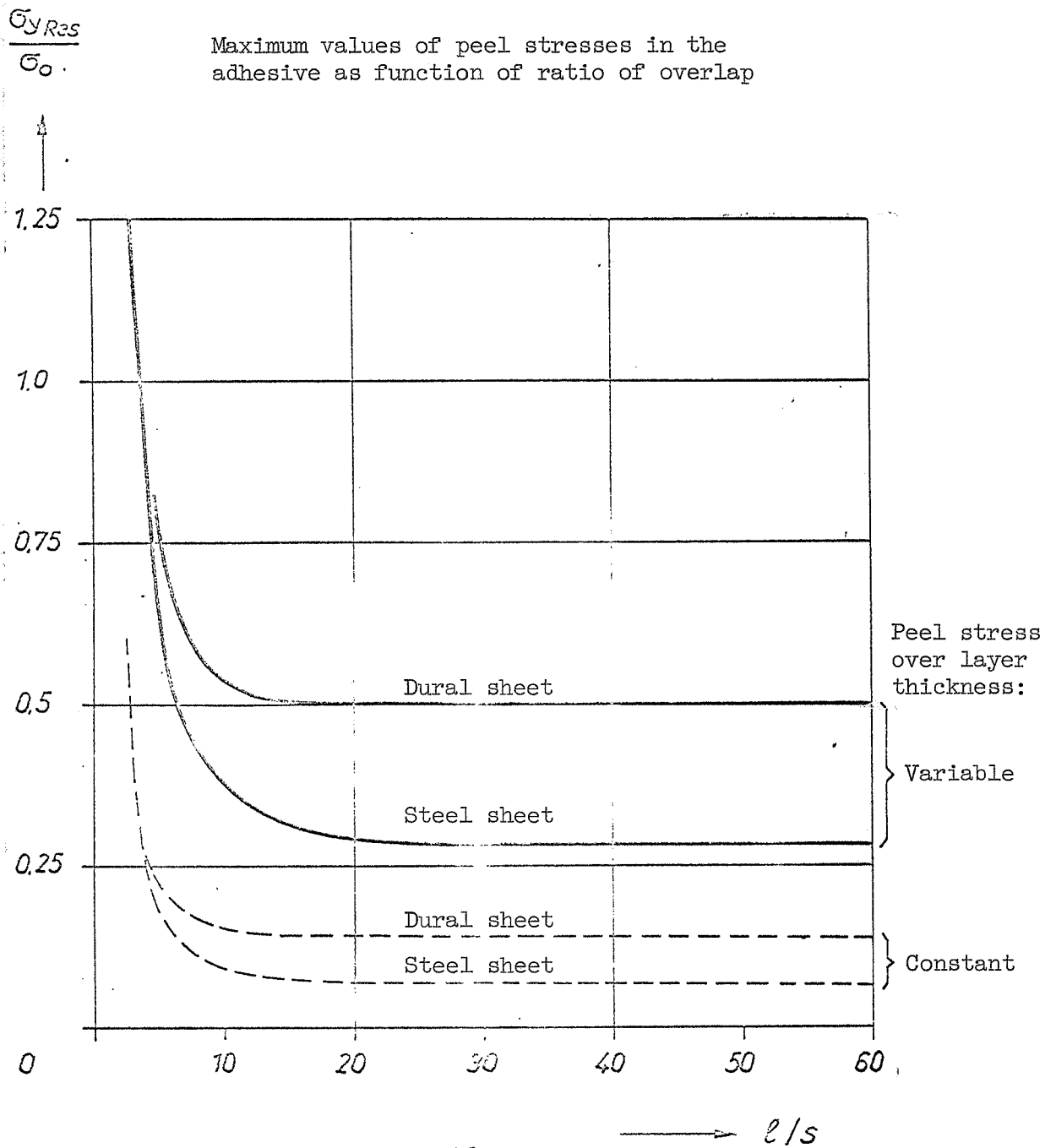


Figure 7

Double-bonded joint: $s = 0.8 \text{ mm}$
 Synthetic resin adhesive: $s_L = 0.2 \text{ mm}$

Maximum peel stresses at the point end

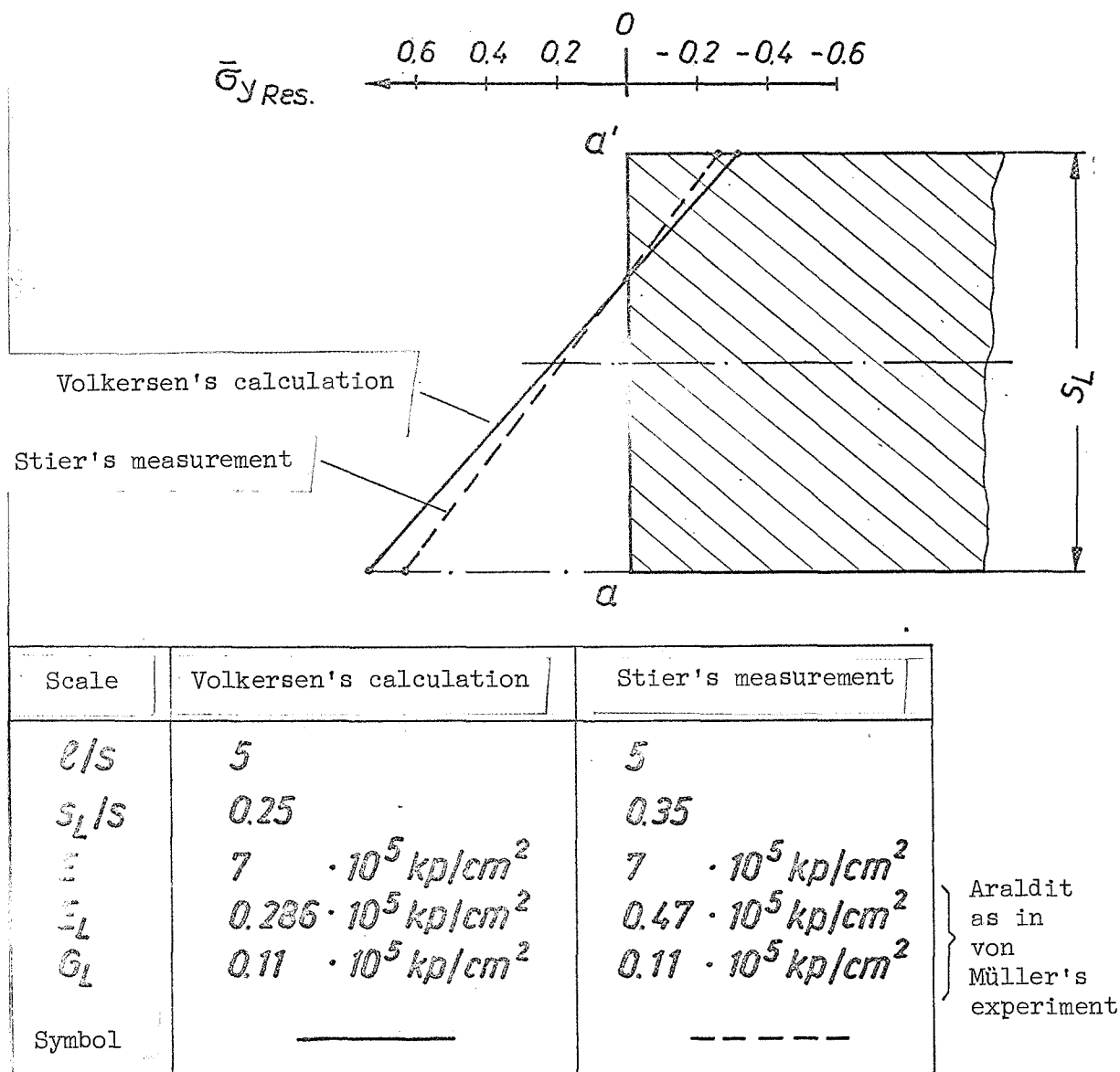


Figure 8. Tension-loaded symmetrical double-bond joint